



Learning Adaptive Total Variation Priors for Variational Image Restoration

Guangyu Yang

School of Automation, Qingdao University, Qingdao 266071, China

* Corresponding Author: **Guangyu Yang**

Article Info

P-ISSN: 3051-3383

E-ISSN: 3051-3391

Impact Factor (RSIF): 8.40

Volume: 07

Issue: 01

Received: 19-12-2025

Accepted: 30-01-2026

Published: 15-02-2026

Page No: 106-115

Abstract

This paper presents an interpretable image restoration framework based on primal-dual variational learning. Different from conventional total variation models with fixed regularization structures, the proposed method introduces learnable anisotropic priors constructed through trainable filtering operators and nonlinear influence functions. A primal-dual optimization strategy is employed to transform the variational model into an efficient trainable architecture, enabling adaptive parameter learning while preserving the interpretability of model-based restoration. To facilitate stable optimization, a differentiable projection mechanism is further incorporated into the learning process. Experimental results on image denoising and image deblurring benchmarks demonstrate that the proposed framework achieves superior restoration performance compared with several representative variational and learning-based methods. The learned regularization priors further provide meaningful interpretations of image structures, illustrating the effectiveness of combining primal-dual optimization with adaptive prior learning.

DOI: <https://doi.org/10.54660/IJAIET.2026.7.1.106-115>

Keywords: image restoration, total variation learning, variational neural networks, bilevel optimization

1. Introduction

Image restoration aims to recover high-quality images from degraded observations and plays an important role in computer vision, computational imaging, and signal processing. Typical restoration tasks include image denoising, image deblurring, compressed sensing reconstruction, and image inpainting. Since the degradation process is usually accompanied by information loss and noise contamination, image restoration is commonly formulated as an ill-posed inverse problem whose solution heavily relies on appropriate prior knowledge of natural images^[1-3].

Variational methods have long been regarded as an effective framework for image restoration. By integrating a data-fidelity term with regularization priors, variational models provide a mathematically interpretable formulation for solving inverse problems. Among various regularization techniques, total variation (TV) regularization has attracted considerable attention because of its ability to preserve image edges while suppressing noise^[4]. To overcome the limitations of the classical TV model, numerous extensions have been proposed, including weighted TV, nonlocal TV, higher-order TV, and total generalized variation (TGV) models^[5-8]. Although these approaches improve restoration quality, most of them still rely on handcrafted regularization functions and predefined prior assumptions, which restrict their adaptability to complex image structures.

The optimization of TV-based models usually leads to large-scale nonsmooth problems. To efficiently solve such models, a variety of optimization algorithms have been developed, including proximal gradient methods, ADMM, forward-backward splitting schemes, and primal-dual algorithms^[9-12]. Among them, primal-dual methods have received increasing attention due to their favorable convergence properties and flexibility in handling nonsmooth regularization terms. In particular, the primal-dual framework proposed by Chambolle and Pock has become a representative optimization tool for variational image restoration and has inspired numerous extensions in imaging applications^[13-16]. In recent years, deep learning has significantly advanced the performance of image restoration. Convolutional neural networks, transformer architectures, and diffusion models have achieved remarkable results on various benchmark datasets^[17,18].

Nevertheless, many deep learning approaches behave as black-box models and often lack explicit physical interpretation.

To bridge the gap between model-driven optimization and data-driven learning, deep unfolding techniques have been introduced by transforming iterative optimization algorithms into trainable neural network architectures [19,20]. Representative methods, including LISTA, TNRD, ADMM-Net, and variational networks, demonstrate that optimization-inspired learning frameworks can achieve both interpretability and competitive restoration performance [21–25].

Despite these advances, several challenges remain. Most existing unfolding methods adopt fixed regularization structures inherited from traditional variational models, limiting their ability to characterize complex image features. Meanwhile, the integration of learnable image priors with primal-dual optimization frameworks remains insufficiently explored. From the perspective of image modeling, natural images contain diverse structures such as edges, textures, and geometric patterns that are difficult to capture using handcrafted regularization functions. The Fields of Experts (FoE) model provides a flexible mechanism for learning image priors through trainable filtering operators and nonlinear influence functions, offering a promising alternative to conventional TV regularization [26,27].

Motivated by the above observations, this paper proposes a primal-dual variational learning framework with learnable total variation priors for image restoration. Specifically, adaptive anisotropic regularization terms are constructed using trainable convolutional operators and nonlinear influence functions. A primal-dual optimization strategy is employed to derive an interpretable trainable architecture, while a differentiable projection mechanism is introduced to improve optimization stability during learning. Experimental results on image denoising and image deblurring benchmarks demonstrate that the proposed framework achieves competitive restoration performance while maintaining strong interpretability.

The main contributions of this work are summarized as

follows:

1. A primal-dual variational learning framework is proposed for image restoration, providing an interpretable integration of variational optimization and deep learning.
2. A learnable anisotropic TV prior is developed using trainable filtering operators and nonlinear influence functions to adaptively characterize complex image structures.
3. A differentiable projection mechanism is introduced to improve optimization stability and facilitate efficient end-to-end parameter learning.
4. Extensive experiments demonstrate the effectiveness and robustness of the proposed approach for image restoration tasks.

2. Proposed Method

The Introduction has highlighted that conventional variational restoration models provide strong interpretability but usually depend on handcrafted regularization terms and manually selected optimization parameters. Although recent unfolding networks have significantly improved restoration performance, many existing approaches still employ fixed regularization structures, limiting their ability to characterize diverse image patterns. To overcome these limitations, we develop a primal-dual variational network with learnable total variation priors. The proposed framework combines adaptive prior learning, primal-dual optimization, and network unfolding within a unified trainable architecture. The overall structure of the proposed framework is illustrated in Fig. 1. Given a degraded image, the network first extracts learnable regularization responses through multiple trainable differential operators. These responses are then incorporated into the primal-dual optimization process, where the primal image variable and the dual regularization variables are alternately updated. By unfolding the iterative optimization procedure into a finite number of stages, the proposed model forms an interpretable trainable network for image restoration.

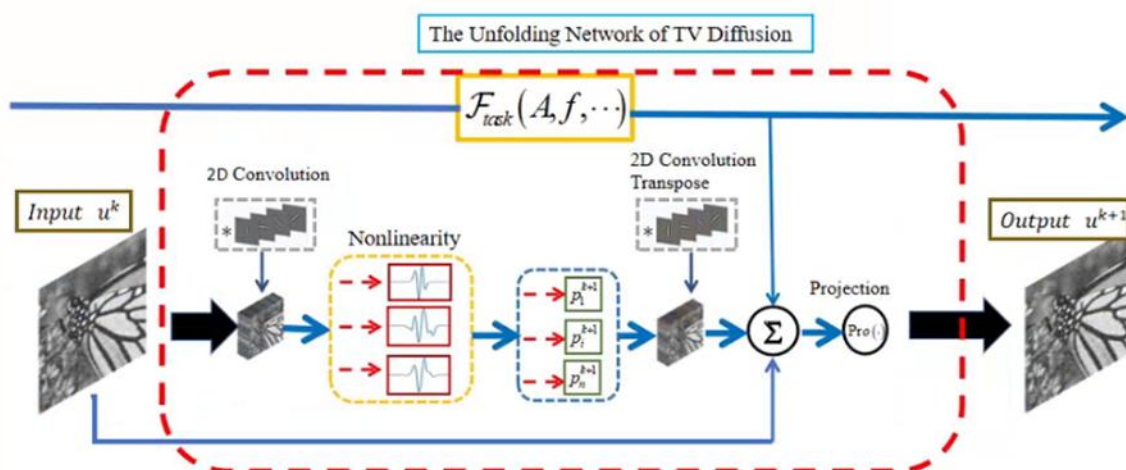


Fig 1: Overall architecture of the proposed primal-dual variational network.

2.1. Variational Restoration Model

Image restoration can be viewed as an inverse problem in which a latent image is recovered from degraded observations. Let u denote the observed image and x represent

the degradation operator. The restoration process is formulated as the minimization of an energy functional consisting of a fidelity term and a regularization term,

$$u = \underset{u}{\operatorname{argmin}} \frac{1}{2} \|Au - f\|_2^2 + \sum_{i=1}^n \gamma_i \|D_i u\|_1 \quad (1)$$

where u denotes the unknown image to be estimated, D_i represents the i -th differential operator, and γ_i controls the contribution of each regularization component.

Different from conventional TV models that mainly rely on first-order derivatives, the proposed formulation allows multiple differential operators to be jointly incorporated into the regularization process. Consequently, structural information at different scales and orientations can be simultaneously captured. Such a design improves the ability of the model to preserve edges, suppress artifacts, and recover fine image details.

2.2. Learnable Total Variation Prior

The restoration quality of variational models largely depends on the effectiveness of the adopted image prior. Traditional TV regularization employs predefined penalty functions, which may not sufficiently describe the statistical characteristics of natural images. To enhance the flexibility of the prior model, a learnable regularization framework is introduced.

Following the Fields of Experts paradigm, the regularization term is represented as $\sum_r k_r \|D_r u\|_1$, where k_r represents the corresponding influence function. Through the combination of multiple filter responses and nonlinear transformations, the proposed regularizer can adaptively model diverse image structures.

To improve parameter efficiency, each filter is constructed as a linear combination of DCT basis functions,

$$k_i = \sum_r \frac{\omega_{i,r} b_r}{\|\omega_i\|_2} \quad (2)$$

where b_r denotes the DCT basis and ω_i is the associated trainable coefficient. This parameterization not only reduces the number of free variables but also provides a stable initialization strategy for network training.

2.3. Primal-Dual Unfolding Optimization

The optimization problem in (1) contains nonsmooth regularization terms, making direct minimization difficult. Instead of applying conventional gradient-based iterations, a primal-dual strategy is adopted. By introducing dual variables associated with the regularization term, the original optimization problem can be reformulated into a saddle-point problem,

$$\begin{aligned} & (u^{k+1}, p_i^{k+1}) \\ & = \arg \max_{\|p_i\| \leq \gamma_i} \min_{u, p} \left(\frac{1}{2} \|Au - f\|_2^2 + \sum_{i=1}^n \langle D_i u, p_i \rangle \right) \end{aligned} \quad (3)$$

This formulation separates the data fidelity term and the TV regularization term into primal and dual optimization components. Therefore, the original problem can be solved by alternating between the dual-variable update and the primal-variable update.

First, when the current restored image u^k is fixed, the dual variable p_i^k is updated by accumulating the response of the differential operator D_i :

$$p_i^{k+1} = p_i^k + D_i u^k. \quad (4)$$

This step extracts the regularization response from the current image estimate and transfers it to the dual space. Since the dual variable is constrained by $\|p_i\| \leq \gamma_i$, a projection operation is then applied to keep p_i^{k+1} within the feasible set.

Second, with the updated dual variable p_i^{k+1} , the primal variable u^{k+1} is updated by combining the gradient of the data fidelity term and the feedback from the regularization term:

$$u^{k+1} = u^k - A^T (Au^k - f) + \sum_{i=1}^n \tilde{D}_i^T D_i p_i^{k+1} \quad (5)$$

Here, $A^T (Au^k - f)$ corresponds to the data fidelity correction, while the summation term represents the contribution of all learnable TV regularization channels. Through this alternating optimization process, the primal variable u^k and the dual variables p_i^k are iteratively refined.

In the unfolding network, each primal-dual iteration is regarded as one network stage. Specifically, one stage consists of four operations: dual-variable update, primal-variable update, projection of the dual variable, and normalization of the restored image. By stacking multiple stages, the iterative optimization process is transformed into a trainable network architecture. The parameters γ_i , ω_i , and related nonlinear functions are learned from training data, while the overall structure remains consistent with the primal-dual optimization process. The detailed structure of one unfolding stage is shown in Fig. 2. Each stage contains dual-variable update, primal-variable update, dual projection, and image normalization modules.

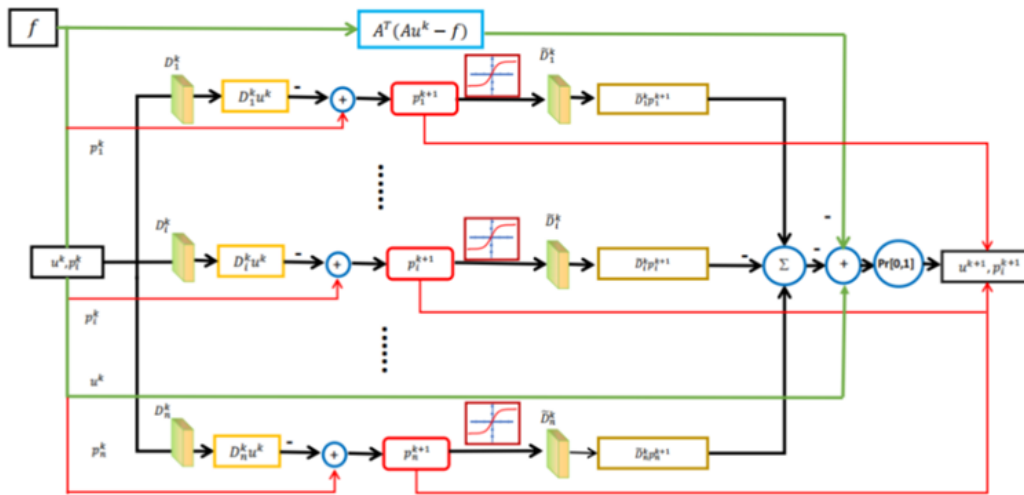


Fig 2: Structure of one primal-dual unfolding stage

2.4. Smooth Projection and End-to-End Learning

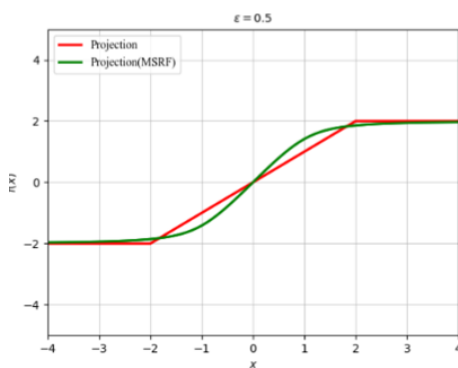
Constraint projection plays an important role in primal-dual optimization. The conventional projection operator is defined as

$$\text{Projection}_\lambda(x) = \begin{cases} -\lambda & x \leq -\lambda \\ x & -\lambda < x < \lambda \\ \lambda & x \geq \lambda \end{cases} \tag{6}$$

Although effective, the above operator contains nondifferentiable points that may hinder gradient propagation during network training.

To address this issue, a smooth approximation is introduced using a regularized Heaviside function which is approximated by a sigmoid function,

$$\text{Projection}_\lambda(x) = \lambda H(x - \lambda) - \lambda(1 - H(x + \lambda)) + x(H(x + \lambda) - H(x - \lambda))$$



(a) projection function

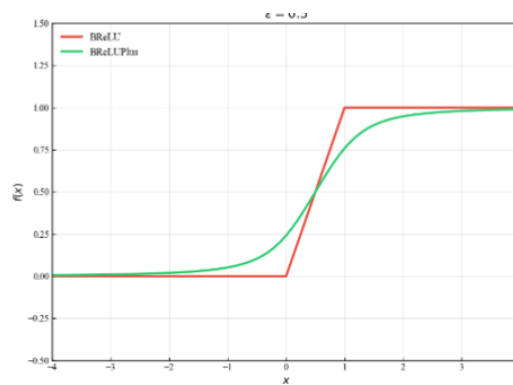
$$\tag{7}$$

which maintains the projection behavior while providing a differentiable computational path.

Similarly, image normalization is implemented through the smooth BReLUPlus function

$$\text{BReLUPlus}(x) = \frac{1}{2} (1 + |x|_\delta - |x-1|_\delta) \tag{8}$$

where δ is a small positive parameter. The proposed activation function improves numerical stability and facilitates efficient network training. Fig. 3 illustrates the original projection function and its smooth approximation. The smoothed form preserves the constraint behavior while avoiding nondifferentiable points, which is beneficial for stable backpropagation in the unfolded network.



(b) BReLU function

Fig 3: Comparison between the projection function and BReLU with their smooth forms

2.5. Network Training

After unfolding the primal-dual optimization process into a finite number of stages, the resulting iterative scheme can be interpreted as a trainable neural network. Each unfolding stage corresponds to one primal-dual update cycle, while the associated model parameters are optimized directly from

training data.

Let Θ encompass penalty coefficients, auxiliary learnable hyperparameters and linear filtering kernels. These parameters are shared within each unfolding stage and jointly optimized during training.

Assume that the network consists of N unfolding stages. Given

a degraded image \tilde{u} . The network parameters are learned by minimizing the discrepancy between the reconstructed image and its corresponding ground-truth image u . The training objective is defined as

$$\Theta = \arg \min_{\Theta} \sum_{s=1}^S \|F(f^s; \Theta) - u^s\| \quad (9)$$

By minimizing the above loss function, the network simultaneously learns image priors and optimization parameters in a data-driven manner. Unlike conventional variational methods that require manual parameter tuning, the proposed framework automatically adapts the regularization strength and filtering operators according to the statistical characteristics of training images.

The gradients of all trainable parameters are computed through backpropagation over the unfolded network. Since the projection and normalization operators are replaced by differentiable approximations, gradient information can be propagated through all unfolding stages without interruption. Consequently, the entire framework can be optimized in an end-to-end fashion.

The proposed training strategy preserves the interpretability of variational optimization while introducing the flexibility of data-driven learning. As a result, both restoration performance and model adaptability are significantly improved.

3. Experiments

3.1. Experimental Settings

To evaluate the effectiveness of the proposed method, experiments were conducted on both image denoising and image deblurring tasks. All experiments were implemented using PyTorch and trained on an NVIDIA GPU platform.

For image denoising, Gaussian noise with different noise levels was added to clean images to generate degraded observations. The BSD68 benchmark was adopted for quantitative evaluation. For image deblurring, standard motion blur kernels and Gaussian blur kernels were employed to generate blurred images. The evaluation datasets include commonly used benchmark images and public

restoration datasets.

Following previous unfolding-based restoration methods, the number of unfolding stages was fixed during training and testing. The trainable parameters include convolutional filters, influence functions, regularization coefficients, and projection parameters. The Adam optimizer was employed for parameter optimization.

Restoration performance was quantitatively evaluated using Peak Signal-to-Noise Ratio (PSNR) and Structural Similarity Index Measure (SSIM). Higher PSNR and SSIM values indicate better restoration quality.

3.2. Analysis of the Proposed Network

To better understand the behavior of the proposed framework, we analyze the learned filters, influence functions, and convergence characteristics of the network.

The filters learned by the proposed framework are visualized in Fig. 4. Different filters exhibit distinct directional and frequency-selective properties, indicating that the network automatically captures meaningful image structures from training data. Compared with handcrafted TV operators, the learned filters provide significantly richer feature representations.

Fig. 5 illustrates several learned influence functions. Unlike conventional convex penalty functions, the learned influence functions exhibit adaptive nonlinear behaviors, allowing the model to better preserve image details while suppressing noise. The learned influence functions shown in Fig. 5 exhibit significantly different shapes from conventional handcrafted regularization functions. Such adaptive nonlinear responses enable the proposed model to capture diverse image structures and textures under different restoration scenarios. The results indicate that the proposed framework automatically learns task-dependent regularization behaviors from data, providing stronger modeling flexibility than traditional TV-based approaches.

The convergence behavior of the proposed network is shown in Fig. 6. As the unfolding stage number increases, restoration performance gradually improves and eventually reaches a stable state. This result demonstrates the effectiveness of the proposed primal-dual optimization strategy.

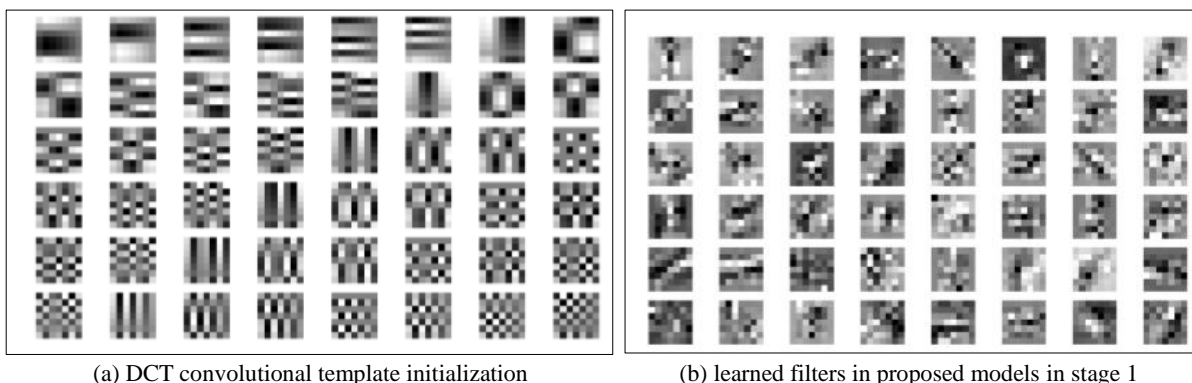


Fig 4: Learned convolutional filters after network training

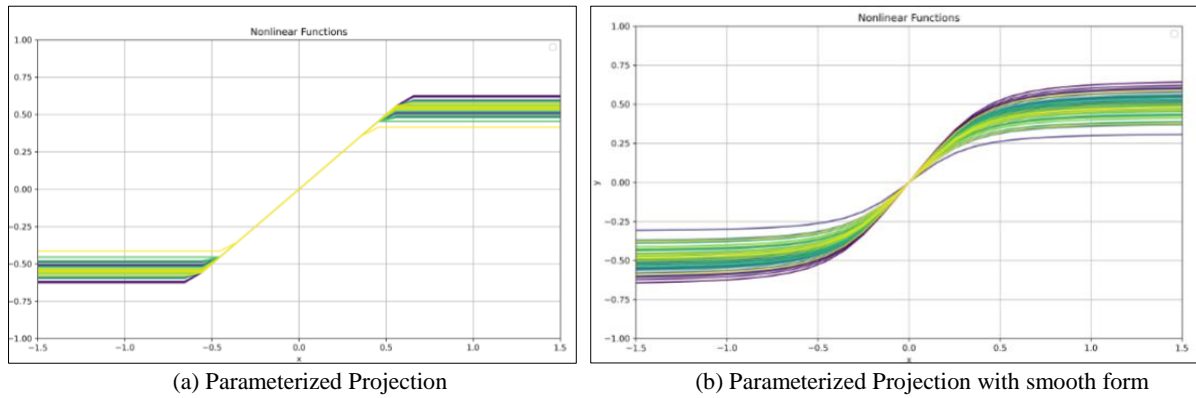


Fig 5: Learned nonlinear influence functions

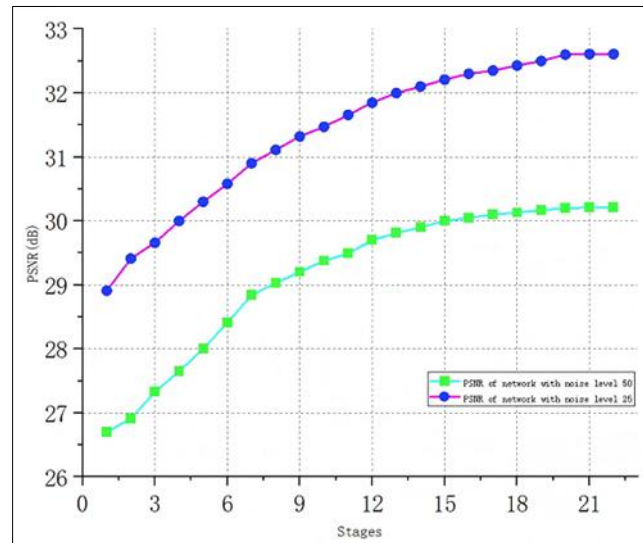


Fig 6: Influence of unfolding stages on restoration performance

3.3. Image Denoising Results

To evaluate the denoising capability of the proposed framework, extensive experiments were conducted on both grayscale and color image benchmarks under different Gaussian noise levels. The proposed method was compared with several representative image restoration approaches, including BM3D [28], TNRD [20], IRCNN [15], and AC-TNRD [30]. Quantitative performance was evaluated using the Peak Signal-to-Noise Ratio (PSNR) and Structural Similarity Index Measure (SSIM).

Representative grayscale image denoising results are presented in Fig. 7. Compared with existing approaches, the proposed method produces cleaner homogeneous regions and sharper edge structures. Although BM3D and TNRD can recover major image features, residual artifacts and detail loss can still be observed around highly textured regions. IRCNN achieves competitive restoration quality through deep feature learning; however, slight structural distortions remain visible in challenging areas. By contrast, the proposed framework preserves more faithful local textures and edge information, demonstrating the effectiveness of the learned total variation prior.

Fig. 8 presents a representative color image denoising

example from the CBSD68 dataset under noise level $\sigma = 50$. Compared with competing methods, the proposed framework produces cleaner homogeneous regions while preserving sharper object boundaries and more accurate color transitions. Benefiting from the adaptive filtering operators and learned nonlinear regularization functions, the restored image exhibits fewer color artifacts and better texture fidelity. These visual results demonstrate that the proposed framework can effectively extend from grayscale image restoration to more challenging color image denoising tasks. To further validate the effectiveness of the proposed framework on color image restoration, quantitative evaluations were conducted on the CBSD68 dataset. The results are summarized in Table 1. The proposed method consistently achieves the highest PSNR values across all tested noise levels. In particular, the performance advantage becomes more evident under severe noise corruption ($\sigma = 50$), indicating that the learned regularization model possesses strong robustness and generalization capability. These results further confirm that the proposed adaptive TV prior can effectively exploit both structural and chromatic information for color image denoising.

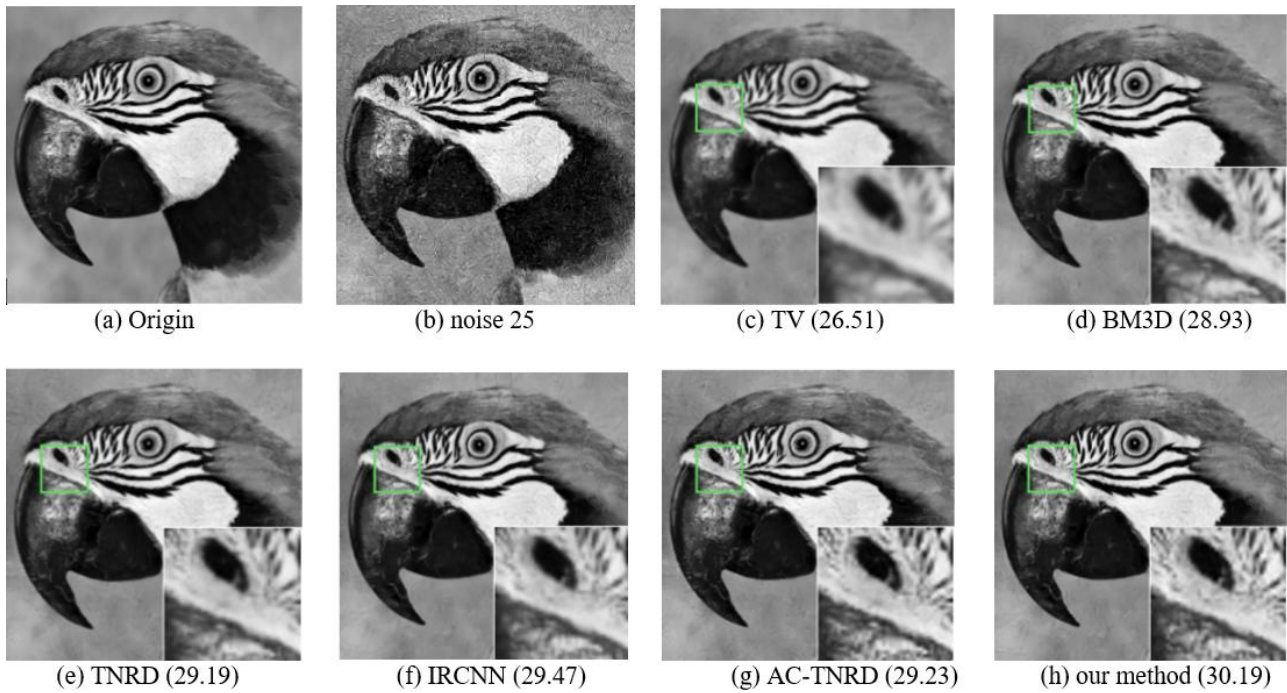


Fig 7: Visual comparison of denoising results for images corrupted by Gaussian noise ($\sigma = 25$).

Table 1: Average PSNR results of denoising on CBSD68 dataset

Methods	CBM3D	TNRD	IRCNN	AC-TNRD	Proposed
$\sigma=15$	33.31	33.79	33.87	33.84	33.90
$\sigma=25$	30.53	31.07	31.18	31.11	31.22
$\sigma=50$	27.42	27.80	27.88	27.82	28.05

3.4. Image Deblurring Results

To further evaluate the generalization capability of the proposed framework, additional experiments were conducted on image deblurring tasks. Unlike image denoising, image deblurring requires simultaneously recovering structural details and suppressing artifacts introduced by the blur degradation process, making it a more challenging restoration problem.

Representative visual comparisons are presented in Fig. 9. The test image contains abundant edge and texture information, providing a challenging scenario for image reconstruction. As observed from the enlarged regions, the restoration result obtained by TNRD still exhibits noticeable loss of local structural details. In contrast, the proposed framework is able to recover clearer edge boundaries and finer texture patterns. In particular, the thin leaf structures highlighted in the zoomed regions are reconstructed more

faithfully, indicating that the learned regularization model can better preserve high-frequency image information during the restoration process.

Quantitatively, the proposed method achieves a PSNR value of 28.58 dB, outperforming TNRD (28.23 dB). Although the numerical improvement is relatively moderate, the visual quality enhancement is more evident. The restored image produced by the proposed framework exhibits sharper structural details and improved local contrast, leading to a more natural appearance.

The above results demonstrate that the learned adaptive TV prior is not limited to denoising applications. By integrating trainable filtering operators and primal-dual optimization, the proposed framework can effectively characterize image structures under different degradation models and achieve robust restoration performance for image deblurring tasks.

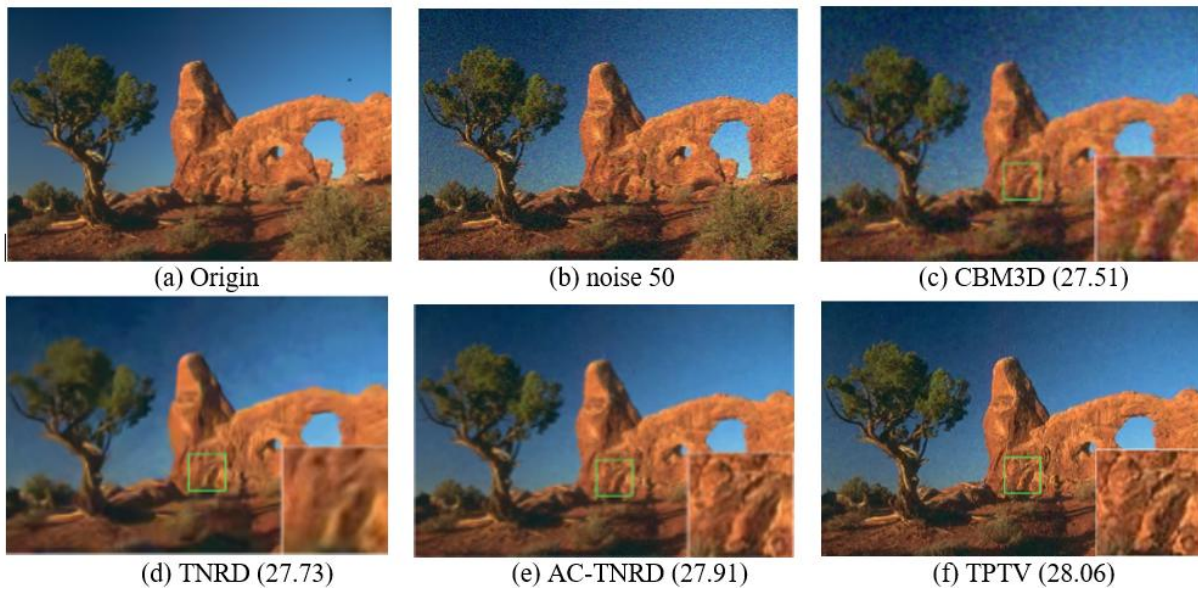


Fig 8: Color image denoising images and PSNR(dB) on Building image from CBSD68 dataset for noise level 50

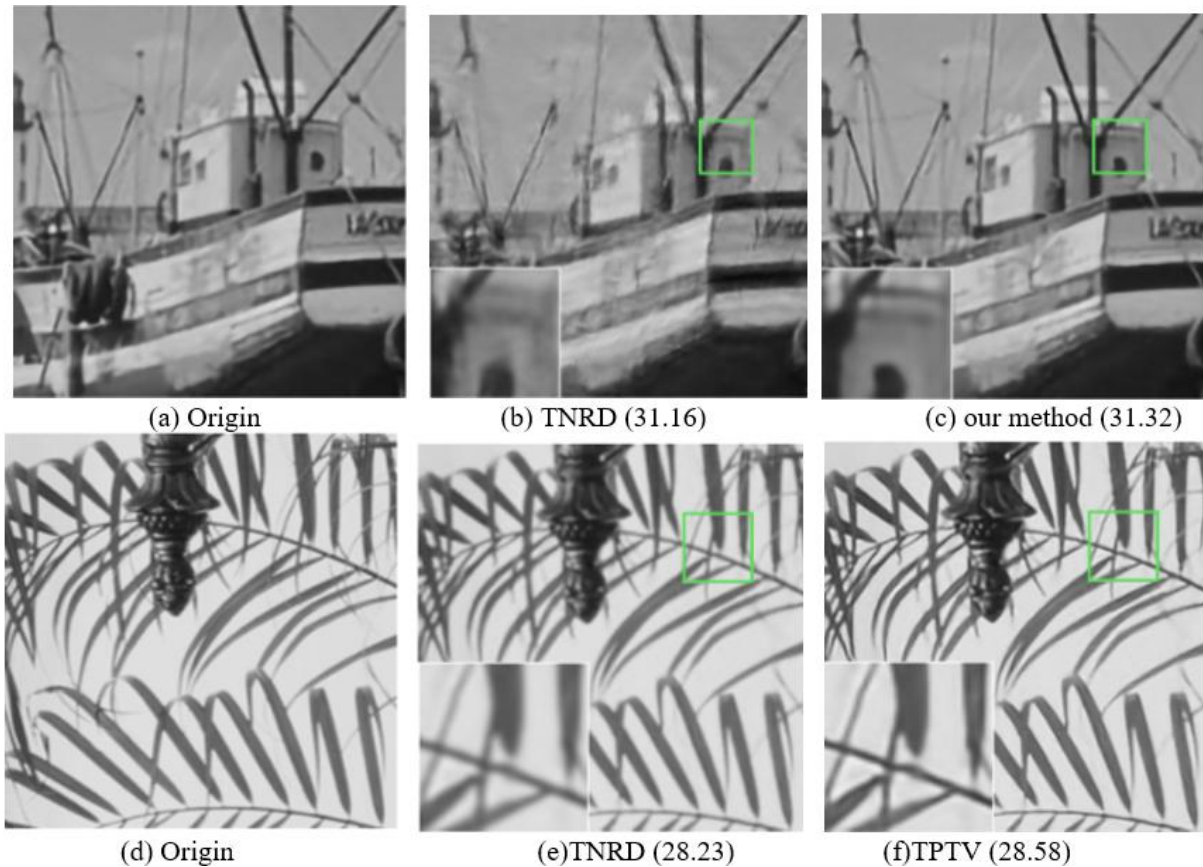


Fig 9: The results of deblurring in Set10 dataset

3.5. Efficiency Analysis

In addition to restoration accuracy, computational efficiency is an important consideration for practical image restoration applications. Since the proposed framework is derived from a finite-stage primal-dual unfolding strategy, its complexity is closely related to the number of unfolding stages and the parameterization of the learnable regularization operators. Table 2 reports the complexity comparison among different restoration methods. Although the proposed framework contains 20 unfolding stages, each stage introduces only 21K trainable parameters owing to the compact DCT-based filter representation and the structured primal-dual architecture.

Consequently, the overall model contains 420K parameters, which is substantially smaller than DnCNN (665K parameters) while achieving comparable restoration performance. The results indicate that the proposed framework maintains a favorable balance between model capacity and restoration accuracy.

To further evaluate computational efficiency, runtime comparisons under different image resolutions are reported in Table 3. For learning-based approaches, both CPU and GPU execution times are provided. The proposed method consistently achieves lower runtime than DnCNN across all image resolutions. For example, on a 1024×1024 image, the

proposed framework requires 4.42 s on CPU and only 0.083 s on GPU, compared with 14.10 s and 0.235 s for DnCNN, respectively. Similar advantages can also be observed for 256×256 and 512×512 images. These results demonstrate that the proposed unfolding architecture can effectively reduce computational cost while maintaining competitive restoration quality.

Combining the results in Tables 2 and 3, it can be observed that the proposed framework achieves an attractive trade-off among restoration accuracy, model complexity, and runtime efficiency. Benefiting from the learnable TV prior and the interpretable primal-dual unfolding structure, the proposed

method not only delivers competitive restoration performance but also maintains relatively low computational overhead, making it suitable for practical image restoration applications. The favorable complexity characteristics mainly originate from two aspects. First, the DCT-based filter parameterization significantly reduces the number of free parameters in each unfolding stage. Second, the primal-dual optimization structure avoids the excessive depth commonly observed in black-box convolutional restoration networks. Therefore, the proposed framework can achieve competitive restoration performance without introducing a substantial computational burden.

Table 2: Complexity comparison of different restoration methods.

Methods (Layer Numbers)	TNRD (5)	AC-TNRD (5)	DnCNN (20)	Proposed (20)
Parameters per Layer	40K	41K	40K	21K
Total Parameters	200K	202K	665K	420K
PSNR (dB)	26.81	26.88	27.21	27.14

Table 3: Runtime comparison under different image resolutions (CPU/GPU, seconds).

Resolution	BM3D (CPU)	DnCNN-B(CPU/GPU)	Proposed (CPU/GPU)
256×256	0.65	0.90 / 0.016	0.47 / 0.011
512×512	2.85	4.11 / 0.060	1.65 / 0.032
1024×1024	11.89	14.10 / 0.235	4.42 / 0.083

4. Conclusion

This paper presented a primal-dual variational learning framework with adaptive total variation priors for image restoration. By incorporating learnable filtering operators and nonlinear influence functions into a variational optimization model, the proposed method enhances the representation capability of conventional TV regularization.

A primal-dual unfolding strategy was employed to transform the iterative optimization process into a trainable network architecture, while differentiable projection and normalization mechanisms were introduced to facilitate stable end-to-end learning. Consequently, the proposed framework combines the interpretability of model-based optimization with the flexibility of data-driven learning. Experimental results on image denoising and image deblurring tasks demonstrated the effectiveness of the proposed approach in both quantitative and qualitative evaluations.

Beyond the performance improvements, the proposed framework provides an effective bridge between model-driven optimization and data-driven learning. By embedding learnable priors into a principled variational formulation, the resulting network retains interpretability while benefiting from the representation power of deep learning. This combination offers a promising direction for future research on interpretable image restoration models.

References

- Bertero M, Boccacci P. Introduction to inverse problems in imaging. Bristol: Institute of Physics Publishing; 1998.
- Chan TF, Shen J. Image processing and analysis: variational, PDE, wavelet, and stochastic methods. Philadelphia: SIAM; 2005.
- Rudin LI, Osher S, Fatemi E. Nonlinear total variation-based noise removal algorithms. *Physica D*. 1992;60(1-4):259-68.

- Chambolle A, Caselles V, Novaga M, Cremers D, Pock T. An introduction to total variation for image analysis. In: *Theoretical foundations and numerical methods for sparse recovery*. Berlin: De Gruyter; 2010. p. 263-340.
- Bredies K, Kunisch K, Pock T. Total generalized variation. *SIAM J Imaging Sci*. 2010;3(3):492-526.
- Gilboa G, Osher S. Nonlocal operators with applications to image processing. *Multiscale Model Simul*. 2008;7(3):1005-28.
- Dong W, Zhang L, Shi G, Li X. Nonlocally centralized sparse representation for image restoration. *IEEE Trans Image Process*. 2013;22(4):1620-30.
- Combettes PL, Wajs VR. Signal recovery by proximal forward-backward splitting. *Multiscale Model Simul*. 2005;4(4):1168-200.
- Beck A, Teboulle M. A fast-iterative shrinkage-thresholding algorithm for linear inverse problems. *SIAM J Imaging Sci*. 2009;2(1):183-202.
- Boyd S, Parikh N, Chu E, Peleato B, Eckstein J. Distributed optimization and statistical learning via the alternating direction method of multipliers. *Found Trends Mach Learn*. 2011;3(1):1-122.
- Esser E, Zhang X, Chan TF. A general framework for a class of first-order primal-dual algorithms for convex optimization in imaging science. *SIAM J Imaging Sci*. 2010;3(4):1015-46.
- Chambolle A, Pock T. A first-order primal-dual algorithm for convex problems with applications to imaging. *J Math Imaging Vis*. 2011;40(1):120-45.
- Condat L. A primal-dual splitting method for convex optimization involving Lipschitzian, proximable and linear composite terms. *J Optim Theory Appl*. 2013;158(2):460-79.
- Vu BT. A splitting algorithm for dual monotone inclusions involving cocoercive operators. *Adv Comput Math*. 2013;38(3):667-81.
- Zhang K, Zuo W, Gu S, Zhang L. Learning deep CNN

- denoiser prior for image restoration. In: Proceedings of the IEEE Conference on Computer Vision and Pattern Recognition (CVPR); 2017. p. 3929-38.
16. Zhang K, Zuo W, Chen Y, Meng D, Zhang L. Beyond a Gaussian denoiser: residual learning of deep CNN for image denoising. *IEEE Trans Image Process.* 2017;26(7):3142-55.
 17. Zamir SW, Arora A, Khan S, Hayat M, Khan FS, Yang MH, et al. Restormer: efficient transformer for high-resolution image restoration. In: Proceedings of the IEEE Conference on Computer Vision and Pattern Recognition (CVPR); 2022. p. 5728-39.
 18. Ho J, Jain A, Abbeel P. Denoising diffusion probabilistic models. In: *Advances in Neural Information Processing Systems (NeurIPS)*; 2020.
 19. Gregor K, LeCun Y. Learning fast approximations of sparse coding. In: Proceedings of the International Conference on Machine Learning (ICML); 2010. p. 399-406.
 20. Chen Y, Pock T. Trainable nonlinear reaction diffusion: a flexible framework for fast and effective image restoration. *IEEE Trans Pattern Anal Mach Intell.* 2017;39(6):1256-72.
 21. Yang Y, Sun J, Li H, Xu Z. Deep ADMM-Net for compressive sensing MRI. In: *Advances in Neural Information Processing Systems (NeurIPS)*; 2016.
 22. Hammernik K, Klatzer T, Kobler E, Recht MP, Sodickson DK, Pock T, et al. Learning a variational network for reconstruction of accelerated MRI data. *Magn Reson Med.* 2018;79(6):3055-71.
 23. Lefkimmatis S. Universal denoising networks: a novel CNN architecture for image denoising. In: Proceedings of the IEEE Conference on Computer Vision and Pattern Recognition (CVPR); 2018. p. 3204-13.
 24. Monga V, Li Y, Eldar YC. Algorithm unrolling: interpretable, efficient deep learning for signal and image processing. *IEEE Signal Process Mag.* 2021;38(2):18-44.
 25. Roth S, Black MJ. Fields of experts: a framework for learning image priors. In: Proceedings of the IEEE Conference on Computer Vision and Pattern Recognition (CVPR); 2005. p. 860-7.
 26. Schmidt U, Roth S. Shrinkage fields for effective image restoration. In: Proceedings of the IEEE Conference on Computer Vision and Pattern Recognition (CVPR); 2014. p. 2774-81.
 27. Chen Y, Ranftl R, Pock T. Insights into analysis operator learning: from patch-based sparse models to higher-order MRFs. *IEEE Trans Image Process.* 2014;23(3):1060-72.
 28. Dabov K, Foi A, Katkovnik V, Egiazarian K. Image denoising by sparse 3-D transform-domain collaborative filtering. *IEEE Trans Image Process.* 2007;16(8):2080-95.
 29. Dabov K, Foi A, Katkovnik V, Egiazarian K. Color image denoising via sparse 3D collaborative filtering with grouping constraint in luminance-chrominance space. In: Proceedings of the IEEE International Conference on Image Processing (ICIP); 2007. p. 313-6.
 30. Yang G, Wei W, Pan Z. A variational neural network for image restoration based on coupled regularizers. *Multimed Tools Appl.* 2024;83:12379-401.

How to Cite This Article

Hadrovic A. The Vranica Mountain in Bosnia and Herzegovina: Living in a sustainable way. *Int J Multidiscip Res Growth Eval.* 2025 Sep–Oct;6(5):718–758. doi:10.54660/IJMRGE.2025.6.5.718-758.

Creative Commons (CC) License

This is an open access journal, and articles are distributed under the terms of the Creative Commons Attribution-NonCommercial-ShareAlike 4.0 International (CC BY-NC-SA 4.0) License, which allows others to remix, tweak, and build upon the work non-commercially, as long as appropriate credit is given and the new creations are licensed under the identical terms.